Stable Grasp Control With a Robotic Exoskeleton Glove

Teja Vanteddu
Department of Mechanical Engineering,
Virginia Tech,
Robotics and Mechatronics Lab,
Blacksburg, VA 24060
e-mail: tejav@vt.edu

Pinhas Ben-Tzvi[1]
Mem. ASME
Department of Mechanical Engineering,
Virginia Tech,
Robotics and Mechatronics Lab,
Blacksburg, VA 24060
e-mail: bentzvi@vt.edu

An exoskeleton robotic glove intended for patients who have suffered paralysis of the hand due to stroke or other factors has been developed and integrated. The robotic glove has the potential to aid patients with grasping objects as part of their daily life activities. Grasp stability was studied and researched by various research groups, but mainly focused on robotic grippers by devising conditions for a stable grasp of objects. Maintaining grasp stability is important so as to reduce the chances of the object slipping and dropping. But there was little focus on the grasp stability of robotic exoskeleton gloves, and most of the research was focused on mechanical design. A robotic exoskeleton glove was developed as well as novel methods to improve the grasp stability. The glove is constructed with rigidly coupled four-bar linkages attached to the finger tips. Each linkage mechanism has one-DOF (degree of freedom) and is actuated by a linear series elastic actuator (SEA). Two methods were developed to satisfy two of the conditions required for a stable grasp. These include deformation prevention of soft objects, and maintaining force and moment equilibrium of the objects being grasped. Simulations were performed to validate the performance of the proposed algorithms. A battery of experiments was performed on the integrated prototype in order to validate the performance of the algorithms developed.
[DOI: 10.1115/1.4047724]

Keywords: linkage mechanisms, dynamics and exoskelotons, wearable robots

1 Introduction

Exoskeleton gloves are used for various applications including virtual reality, tele-operation, rehabilitation, etc. Exoskeleton gloves have significant potential in the medical field which can assist patients suffering from paralysis in their hands due to stroke and other nerve-related diseases to grasp objects in their daily lives. This paper focuses on the development of algorithms for better control of grasp stability of the exoskeleton glove developed by Refour et al whose detailed design can be found in Ref. [1] and its updated design can be found in Ref. [2].

Exoskeleton gloves can be broadly classified into two main categories: (1) soft gloves and (2) rigid gloves. Soft gloves generally are lightweight, compact, and typically exhibit low motion hindrance. Soft gloves are generally actuated by cables or wire like mechanisms such as cable actuated gloves [3], gloves with soft tendon routing mechanism [4], and Bowden cable system for remote actuation [5]. On the other hand, rigid gloves have better force transmission, low friction loss, and can achieve better grasp configurations. Few examples of rigid gloves developed so far include the SAFER glove which uses Gaussian mixture regression method to generate force trajectories for each of the fingers [6], gloves that can exert high forces using underactuated serial linkage mechanisms [7], and gloves that use a combination of rigid linkages actuated by series elastic actuator (SEA) using Bowden cable mechanisms [8]. The current glove is designed as a rigid glove as shown in Fig. 1. It exhibits attributes such as high force transmission and repeatability but is also compact and lightweight like a soft glove since it uses a 1-DoF (degree of freedom) linkage mechanism for each finger and uses SEA for its actuation. Most of the previous research was heavily focused on the mechanical design and kinematics analyses of the gloves. There was less exploration carried out in the field of control of the gloves and stability of the grasp when the glove is holding an object. This paper is concerned with the stability of the grasp and algorithms were developed to improve grasp stability.

Any robotic gripper or exoskeleton glove needs to apply sufficient forces when grasping objects such that they satisfy the stability conditions as defined by various researchers in Refs. [9–12]. For a grasp to be stable, the forces being applied to the object should satisfy the force and moment equilibrium, and the forces should not be too large so as to prevent deformation of the object and damage to the fingers. Other conditions include slip prevention, but in this research the focus was devoted to the former two considerations, and algorithms were developed to satisfy these two conditions. To the best of the authors' knowledge, most of the work on stable grasping was implemented for robotic grippers and not for exoskeleton gloves.

The exoskeleton glove needs to use all five fingers for grasping objects as it will reduce the amount of force applied by individual fingers except for the thumb and also reduces the chances of the object from slipping and falling [13]. Some research on grasp stability includes grasp stability learning using tactile information, which essentially incorporates sensors all along the robotic hand fingers of a Barret hand. The Barret hand consists of a model that predicts the stability of the grasp based on the tactile information [14]. Nakashima et al have defined conditions for stable grasps and designed a controller for a single finger that satisfies the stability conditions [10]. Work on stable precision grasps was carried out on a two-finger pinch gripper by Kragten et al. [15], where they made mechanical design changes to a gripper linkage so that the grasping stability increases. Multi-fingered gripper stability analysis was carried out by Ref. [16] where they performed stability analysis of a four-fingered gripper grasping a cube oriented such that the forces on the fingers are symmetric. A parallel hybrid hand was designed by Lu et al. [11] where the forces on each finger were determined by optimization so that the forces are as far as possible from the boundary of friction cone, where friction cone is a cone formed by the maximum theoretical friction force vectors about the point of application of the force. But this analysis was performed without considering the mass of the object grasped and only the external forces were taken into account. Maximilian worked on the effect of passive reactions on grippers with stiff and non-back drivable actuators on the stability of a grasp [17]. Bekiroglu et al.
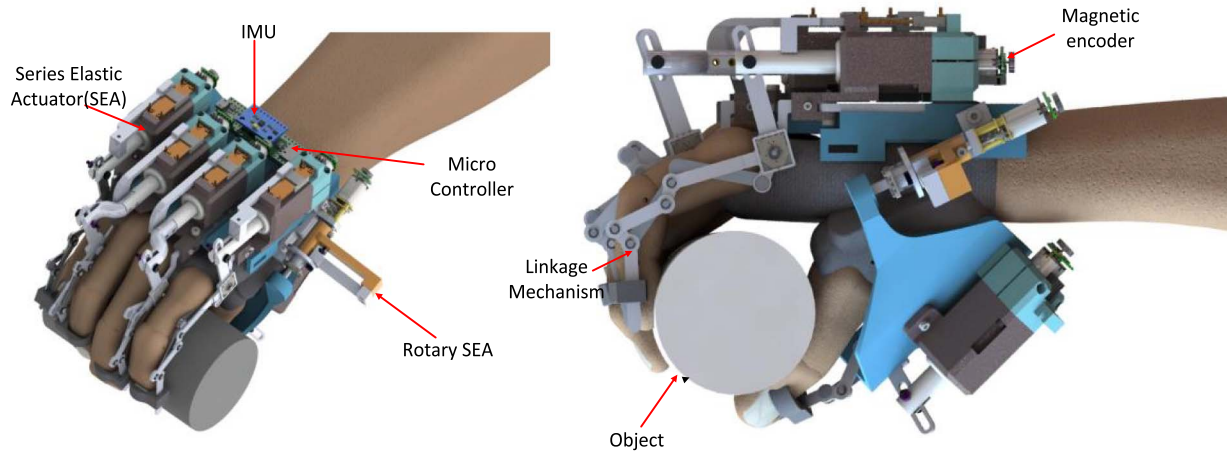
Fig. 1 Exoskeleton glove worn by a hand to grasp a cylindrical object. The exoskeleton glove has a 1-DoF linkage mechanism for each finger and each linkage mechanism is driven by a linear SEA. A spring element is attached in series to the linear actuator thus allowing for measurement of forces being applied to grasped objects.

have developed a method to assess grasp stability based on readings from visual and tactile sensors and implemented a learning framework which was trained using synthetic datasets [12]. Intelligent grasping methods such as slip detection was explored by Ref. [18] where the stability of the grasp was improved by detection of slip and iterative increment of normal contact forces. Chauhan and Ben-Tzvid [19] and Chauhan et al. [20] developed prediction algorithms that can detect minute movements in the fingers and predict the type of grasp intended by the user, which was executed by the exoskeleton glove to completion.

In the field of grasping of deformable objects, Howard and Bekey [21] have trained a neural network algorithm to extract minimum gripping force required for a deformable object whose deformation characteristics are physically modeled. Another neural network based approach was used by Ref. [22] where a vision system was used to monitor the deformation of soft objects, which were correlated to the magnitude of the applied forces. This information was used in a controller to improve the grasp stability of soft objects. A tactile sensor was developed by Ref. [23], whose haptic feedback can be used to differentiate between soft and rigid objects. This sensor can be used on a gripper at the finger tips and the sensor data can be used to apply force based on the soft or rigid object detected. Another method by Ref. [24] uses a vision sensor and other sensor data such as finger position, velocity, and the forces applied, to build a 3D model of the object and its deformation. Delgado et al have developed a control strategy described in Ref. [25], which uses tactile information to adjust its force limits based on the deformability degree calculated for the object. Grasping of soft objects with flexible tools was studied by Ref. [26], where visual information from stereo cameras was used to control the position of the tool tip while making contact with the soft object and neural networks was used to improve the accuracy of the position of the tool. These methods were implemented on robotic grippers and required vision, which not only introduces its own set of limitations such as the need for uniform lighting and no background objects but also increases the on-board computation power required. Since in the case of exoskeleton gloves, the trajectory information is not known prior to the manipulation of the object as it is dependent on the user, there is a need to develop a control method that can detect the change in kinematic the state of the object instantaneously and apply forces accordingly to meet the stability conditions.

The following sections will introduce the mechanical design and the hardware used for testing the prototype through experiments. Section 2 introduces the deformation detection algorithm and provides an explanation of how the algorithm works. Simulation results are shown for the algorithm for various materials with different stiffness. Section 3 discusses the optimal force algorithm where the method of generating an optimal force distribution such that it satisfies the moment and force equilibriums and simulation results are also presented. Sections 4 and 5 describe the developed control architecture and prototype integration, respectively. Section 6 details the experimental results of both the deformation detection algorithm and the optimal force algorithm and the results are analyzed. The paper is concluded with analysis of the results, the novel contributions of this paper and future work that would advance this research further.

2 Deformation Detection Algorithm

As mentioned in Sec. 1, preventing the application of large force to avoid deformation of objects is one of the conditions of a stable grasp. This algorithm was developed to prevent crushing or deforming soft objects by the glove. Initially, when the glove is in noncontact state with the object, the user provides intent to grasp the object either by voice command or some input device such as a mechanical switch. Upon receiving the intent to grasp, the linkages of the glove are driven at certain velocity thus closing toward the object. Since the glove does not know the shape of the object also due to nonlinear relation between the speed of the linear SEA and fingertip velocity, all four fingers may not touch the object at the same time. If the finger that touches the object earlier than other fingers starts applying force then it may cause the object to tilt or fall over. To prevent this, the fingers stop immediately upon detecting the presence of an object and wait until all fingers have made slight contact with the object. After ensuring that all the fingers have made contact, the deformation detection algorithm is initialized. This algorithm takes in as input a predefined force that is applied and sent as the reference signal to the actuators. Before the algorithm is further explained, it is important to describe the sensors that are available on the glove necessary for this process. For each finger, there are two sensors, one is a linear potentiometer and the second is a magnetic hall-effect encoder. The linear potentiometer measures the distance traveled by the end of the spring in the SEA connected to the linkage.

In the algorithm, ω is the motor velocity, F_d is the initial predefined force provided to the algorithm, F_{ref} is the reduced force after detection of deformation, and ΔD_{POT} is the deformation as measured by the linear potentiometer.

The magnetic hall-effect encoder measures the motor position which could be used to measure the linear displacement of the

end of the spring connected to the motor. As the glove applies force on the object, based on the deformation that is calculated based on the difference in sensor readings in the SEA, the force value is reduced online to minimize the deformation of the object. Figure 2 describes the algorithm used for deformation detection. The algorithm initially is in State 1 where the glove is waiting for a user input to initiate grasp which is either through twitch movement or a switch. Once the input is detected, the glove starts flexion motion and the fingers are driven closer to the object. The contact of fingers with the object is detected and the system transitions to State 2. In State 2, the linear potentiometer measurement is being tracked and based on the change in its measurement from the moment the contact is made the initial predefined force is reduce in proportion to the change. The force reduces until there is no change in measurement of the linear potentiometer. The glove continues to apply the new reduced force until the user provides an input to release the grasp. Here it is assumed that the finger stiffness is very high thus its effect on the algorithm is negligible. The finger stiffness can further reduce the required force so tests can be performed to estimate it. This estimate can be used to recalibrate the algorithm so as to take into account the effects of the fingers stiffness.

Before testing the algorithm on a physical prototype, a simulation was performed to test it. For the simulation, the object to be grasped was modeled as a linear spring based on results from the finite element analysis (FEA) simulation performed on a shell type cylindrical object as shown in Fig. 3 with transverse forces applied on the object.

The maximum displacement from the FEA simulation was found to be linearly dependent on the force being applied. The simulation was performed in SIMULINK and was tested on four different object stiffness values. Simple force control algorithm results are used for comparison with that of using the deformation detection algorithm.

In the simple force control, the force is applied in a manner such that it is equal to the predefined force irrespective of the deformation observed. And in the case of the deformation detection algorithm, the reference force is reduced in proportion to the deformation detected. Figure 4 clearly shows a difference between the

deformations when a simple force algorithm is used compared with when a deformation detection algorithm is used. As can be noticed from the results, the deformation reduction is higher for softer objects as compared with stiffer objects. This implies that for rigid objects the algorithm will apply force that is more close to the initial predefined force.

3 Optimal Force Algorithm

As previously described, one of the conditions for a stable grasp is that the glove should apply forces such that the force and moment equilibriums are satisfied.

For the sake of simplicity, only cylindrical grasps were considered since they are the most common in daily life activities. Three points of contact are necessary and sufficient to grasp a 3D object, but while performing cylindrical grasp with the glove, five fingers come in contact with the object. Since there are more contact points than necessary, there will be infinite combinations of force distributions that can satisfy the force and moment equilibriums.

Therefore, an optimization method was used to find the optimal set of force distribution that meets the stability conditions. While grasping the user may move the object in a translational or rotational motion or a combination of both. During this user imparted motion, the forces required to meet the equilibrium conditions also change in a dynamic manner. Therefore, an inertial measurement unit (IMU) is used to measure the real-time kinematic state of the glove which is fed into the optimization algorithm to calculate the optimal set of forces.

3.1 Dynamics Modeling of the Grasp. The dynamics of grasping an object needs to be analyzed which will be used in the optimization as constraint equations. The forces are labeled in Fig. 5 where a human hand wearing the exoskeleton glove is grasping a cylindrical object. Here, various coordinate frames are defined which include the world coordinate system, object coordinate system, and glove coordinate system. The contact forces are related by Eq. (1) where it satisfies the force and moment equilibrium
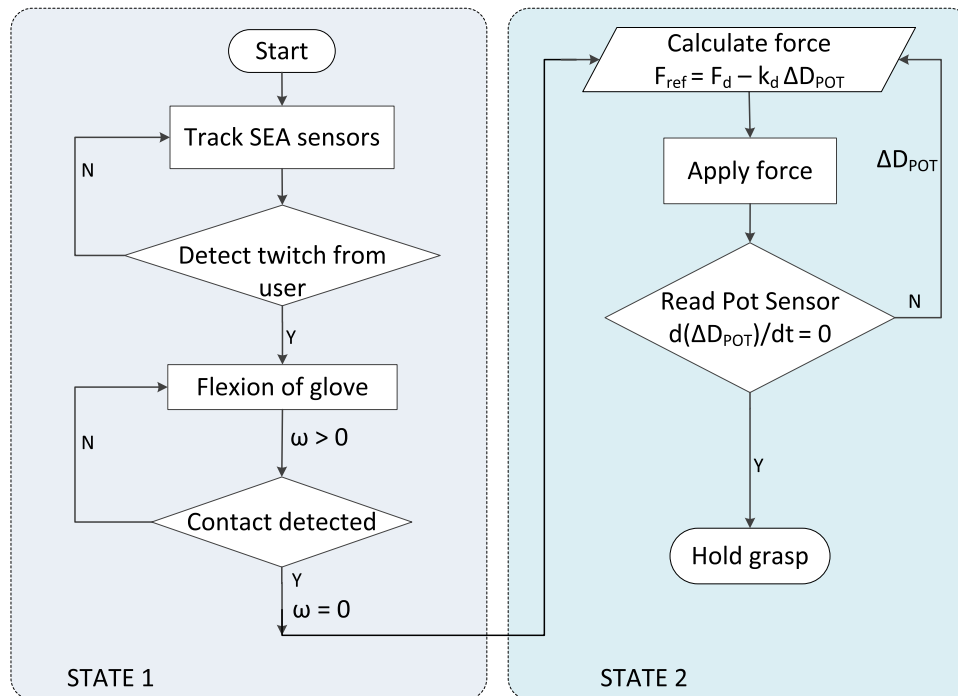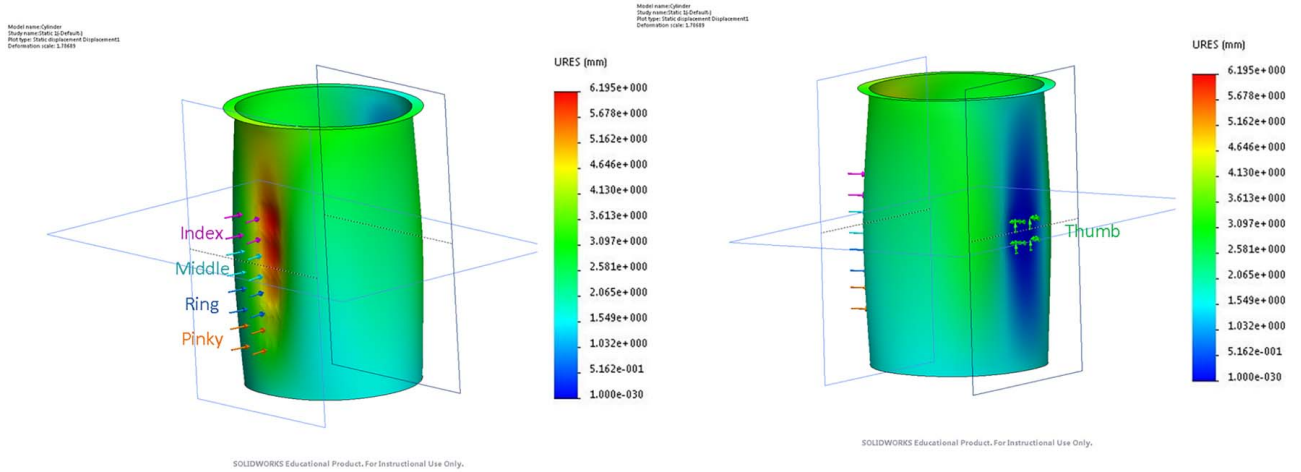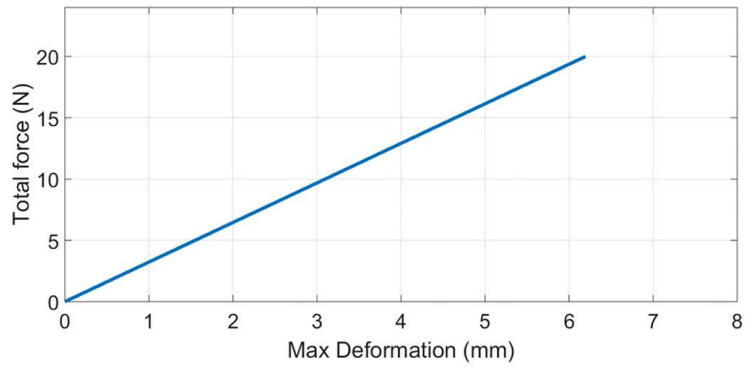

Fig. 2 Flowchart describing the deformation detection algorithm. There are two states for the system, initially in State 1 the glove is in grasping stage and in State 2, deformation is measured by the system and accordingly adjusts the force being applied.

Fig. 3   FEA analysis of thin film cylindrical object. This analysis shows a thin film cylinder and normal forces are applied in FEA software. Upon iteratively increasing the force applied, deformation is found to increase in a linear manner.
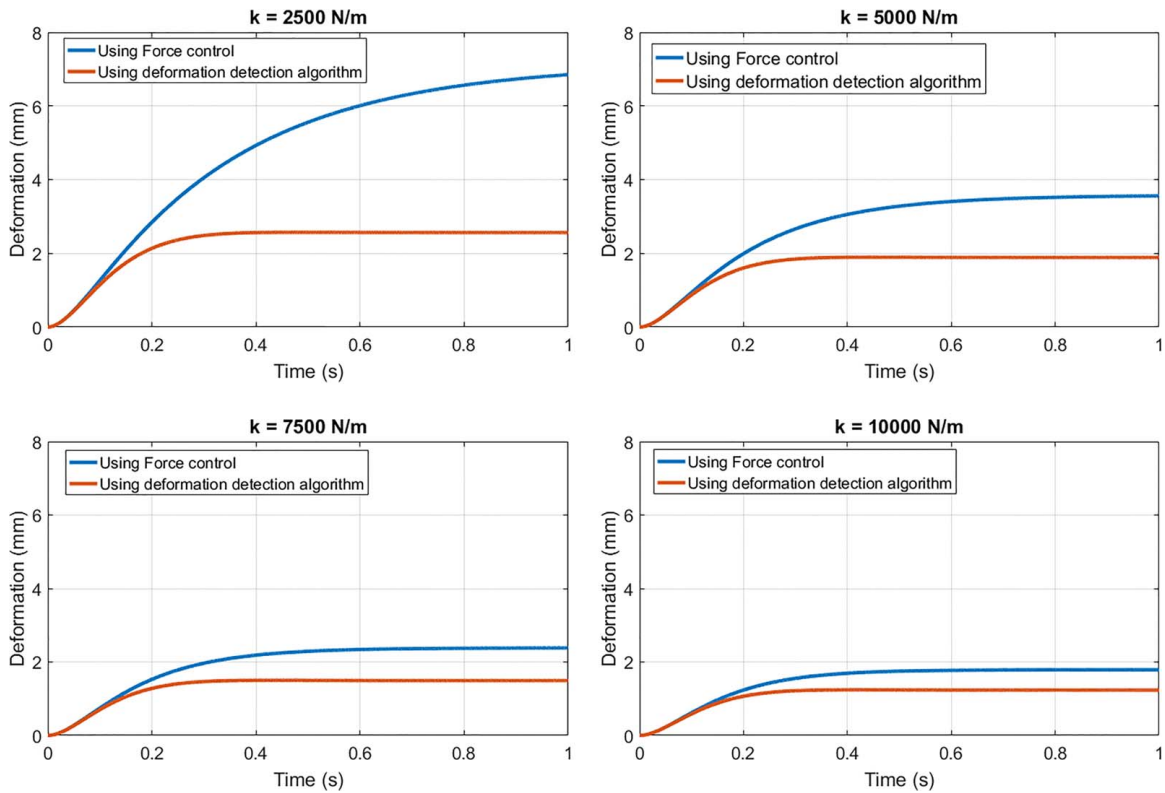
Fig. 4   Comparison plots between using deformation detection algorithm and force control. For this simulation, a linear mass-spring model was used as a model for the object to be grasped. Simulation results are shown for four stiffness values and from observation the algorithm affects the force in larger magnitude for softer objects.
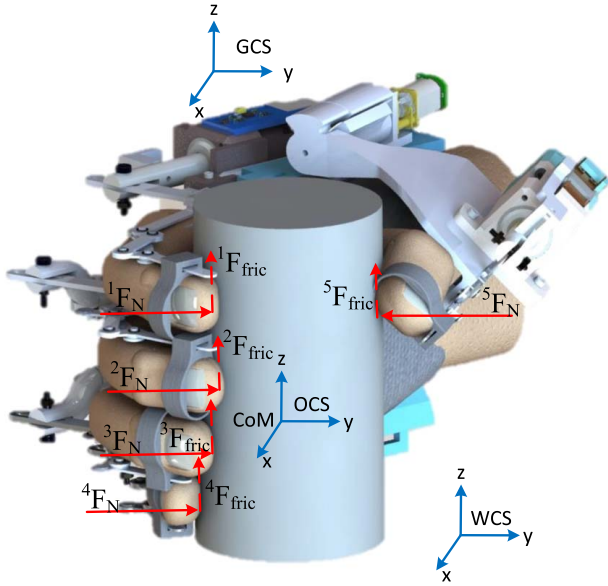
Fig. 5 Forces on the object due to the glove. Here a human hand wearing the exoskeleton glove is holding a cylindrical object and the forces experienced by the object are labeled along with the coordinate frames.

$$\sum_{k=1}^{5} \mathbf{S}_k \mathbf{F}_k + \mathbf{S_{trans}} M \ddot{\mathbf{x}} + \mathbf{S_g} M \mathbf{g} + \mathbf{S_{rot}} I \ddot{\boldsymbol{\theta}} = 0 \qquad (1)$$

where

$$\mathbf{S}_k = \begin{bmatrix} R_{k\_cm} & p_{k\_cm} R_{k\_cm} \\ 0 & R_{k\_cm} \end{bmatrix}$$

$$\mathbf{F}_k = R_{w\_g} R_{g\_f} \begin{bmatrix} {}^k F_N \\ 0 \\ {}^k F_{fric} \end{bmatrix}$$

$$\mathbf{S_{trans}} = \mathbf{S_{rot}} = \begin{bmatrix} R_{imu\_cm} & p_{imu\_cm} R_{imu\_cm} \\ 0 & R_{imu\_cm} \end{bmatrix}$$

$$\ddot{\mathbf{x}} = \begin{bmatrix} a_x \\ a_y \\ a_z \end{bmatrix}, \ddot{\boldsymbol{\theta}} = \begin{bmatrix} \dot{\omega}_x \\ \dot{\omega}_y \\ \dot{\omega}_z \end{bmatrix}$$

where ${}^k F_N$ is the normal force applied by the kth finger on the object, ${}^k F_{fric}$ is the friction force due to the kth finger on the object, R_{k_cm} is the rotation matrix from the point of contact of the kth finger to the center of mass of the object, p_{k_cm} is the translation matrix from the point of contact of the kth finger to the center of mass of the object, R_{k_cm} is the rotation matrix from the IMU to the center of mass of the object, p_{k_cm} is the translation matrix from the IMU to the center of mass of the object. a_x, a_y, and a_z are the linear acceleration along the three axes, ω_x, ω_y, and ω_z are angular velocities of the object along the three axes and these parameters are calculated by the IMU placed on the glove. The above equations satisfy the equilibrium equations as required for meeting one of the stability conditions. Slip is prevented by applying the friction constraint on the forces as given in Eq. (2)

$$\sum_{k=1}^{5} \mu^k F_N \sin(\theta_z) \geq mg + m\ddot{x}_z \qquad (2)$$

where μ is the friction coefficient of the object and θ_z is the orientation of the object with respect to the z-axis. The forces on the fingers ${}^k F_N$ are determined by performing optimization such that they meet the above given stability condition equations.

3.2 Optimization. For any optimization problem, an objective function which will be minimized under given constraints needs to be formulated. For this case, two objective functions are proposed as shown in Eq. (3)

$$f(.) = {}^1 F_N^2 + {}^2 F_N^2 + {}^3 F_N^2 + {}^4 F_N^2 \qquad (3)$$

This is a constrained optimization problem and in this case there is one equality constrained Eq. (1) and one inequality constrained Eq. (2). While performing optimization, there is a possibility for the optimal solution to be out of bounds which cannot be implemented in real life. Therefore, the bounds on each design variable are given in Eq. (4). The lower bound is chosen such that there are no negative values generated which cannot be implemented as the linkage can only apply force in the push direction but not in the pull direction. The upper bound is determined by the maximum actuator force limits

$$0 < \{ {}^1 F_N, {}^2 F_N, {}^3 F_N, {}^4 F_N \} \leq F_{motorLim} \qquad (4)$$

Equation (9) is the optimization problem with the equality and inequality constraints, which are rearranged forms of Eqs. (1), (2), and (4)

$$\min \ f_o = {}^1 F_N^2 + {}^2 F_N^2 + {}^3 F_N^2 + {}^4 F_N^2$$

Subject to $\quad A[x] = b$

$[x] = \begin{bmatrix} {}^1 F_N & {}^2 F_N & {}^3 F_N & {}^4 F_N \end{bmatrix}^T$

$f_i \leq 0, \quad i = 1, 2, 3$

where,

$A = \begin{bmatrix} S_1 & S_2 & S_3 & S_4 \end{bmatrix}$

$b = -(\mathbf{S_{trans}} M \ddot{\mathbf{x}} + \mathbf{S_g} M \mathbf{g} + \mathbf{S_{rot}} I \ddot{\boldsymbol{\theta}})$

$f_1 = \begin{bmatrix} -{}^1 F_N & -{}^2 F_N & -{}^3 F_N & -{}^4 F_N \end{bmatrix}$

$f_2 = \begin{bmatrix} {}^1 F_N - F_{motorLim} & {}^2 F_N - F_{motorLim} & {}^3 F_N - F_{motorLim} & {}^4 F_N - F_{motorLim} \end{bmatrix}$

$$f_3 = mg + m\ddot{x}_z - \sum_{k=1}^{5} \mu^k F_N \sin(\theta_z) \qquad (5)$$

To solve this optimization problem on a microcontroller, we use a barrier method which is an interior point method, the details of which are provided in Ref. [27] used for solving optimization problems with inequality constraints. In the barrier method, inequality constraints are transformed to equality constrained optimization problem as shown in Eq. (6)

$$\min \ f_1 = t(f_0) + \phi(x)$$

Subject to $\quad A[x] = b$

where,

$$\phi(x) = -\sum_{i=1}^{m} \log(-f_i(x)) \qquad (6)$$

where f_1 is the new objective function which includes the inequality constraint and t is a parameter which affects the accuracy. The optimal values are obtained in an iterative manner where the values are updated until they converge to the optimal value.

The equation for updating the x value is described in Eq. (7)

$$\begin{bmatrix} \Delta x \\ w \end{bmatrix} = \begin{bmatrix} \nabla^2 f & A^T \\ A & 0 \end{bmatrix}^{-1} \begin{bmatrix} -\nabla f \\ b - Ax \end{bmatrix} \qquad (7)$$

This method requires a starting point which is feasible such that it satisfies the constraint equations. Therefore, infeasible start Newton method [27] is used simultaneously to find the feasible solution. This method allows any arbitrary point or set of force values as the starting point. The algorithm that calculates the optimal force values using the infeasible start Newton method and the barrier method is detailed in Table 1.

Table 1 Optimal force algorithm

Input : choose arbitrary x such that, $x \ \varepsilon$ dom (f_0) and $f_i(x) < 0$ is satisfied
Input object properties such as mass, inertia etc.
Define parameters like motor limits, distance between linkages
Read IMU data and fetch current acceleration and orientation of the object
Setup : Formulate new objective function f_1 as given in Eq. (6)
Define the equality constraint equation matrices A and b
for $i = 1 : 30$
    1. Find Δx using Eq. (7)
    2. Update $x = x + \Delta x$
    3. Repeat step 1 with updated x value; Update i ++
end
Output : Optimal force values—x

The above algorithm was implemented in MATLAB and all the force values converged approximately in around 30 iterations as shown in Fig. 6 and the algorithm when implemented on teensy 3.6 microcontroller, it took 12 ms to compute 30 iterations.

4 Controls Architecture

The force reference values for each actuator are generated by the optimization algorithm as described in Sec. 3.2. These reference force values are sent to a controller that drives the SEA toward the reference force value. The overall control architecture is shown Fig. 7 where there are five actuators each with their own controller. To design the controller for the SEA, a transfer function of the SEA needs to be derived. Viscous friction was assumed to be present in the actuator. In the transfer function for free motion of the linkage mechanism as given in Eq. (8), the unknown parameters are the viscous friction coefficient b and the Inertia J as observed by the motor

$$\frac{\theta_m}{V} = \frac{k_t}{s^2 JR + s(bR + k_v k_t)} \tag{8}$$

where θ_m is the motor position (rad), R is the motor resistance, k_t is the torque constant of the motor, k_v is the motor velocity constant, J is the effective inertia, and b is the effective viscous coefficient.

Estimation of these two parameters is achieved by using system identification technique. System identification requires input and output data either in the time-domain or the frequency domain based on which the transfer function of the plant is estimated such that it best matches with the output for the given input.

These data are acquired by sending a constant input voltage to the motor and measuring the linear position with respect to time. These data are fed into the system identification application in MATLAB to estimate the transfer function. In Fig. 8, we can observe that the output of the transfer function is approximately matching with the measured output data for all four actuators.

Motor controller is designed based on the estimated transfer functions. The output results of a tuned PID (proportional-integral-derivative) and PI (proportional-integral) controller in SIMULINK were similar so a PI controller was selected for the sake of implementation simplicity. The rise time approximately for all four linkages is around 0.6 s. The PI controller gains are tuned in SIMULINK using PID tuner and the model was built using the transfer function that includes the dynamics of the spring in the linear SEA as given in Eq. (9)

$$\frac{\theta_m}{V} = \frac{k_l}{s^2 JR/k_t + s(bR + k_v k_t)/k_t + Rk_s k_l^2/k_t} \tag{9}$$

$$k_l = \frac{P}{2\pi N}$$
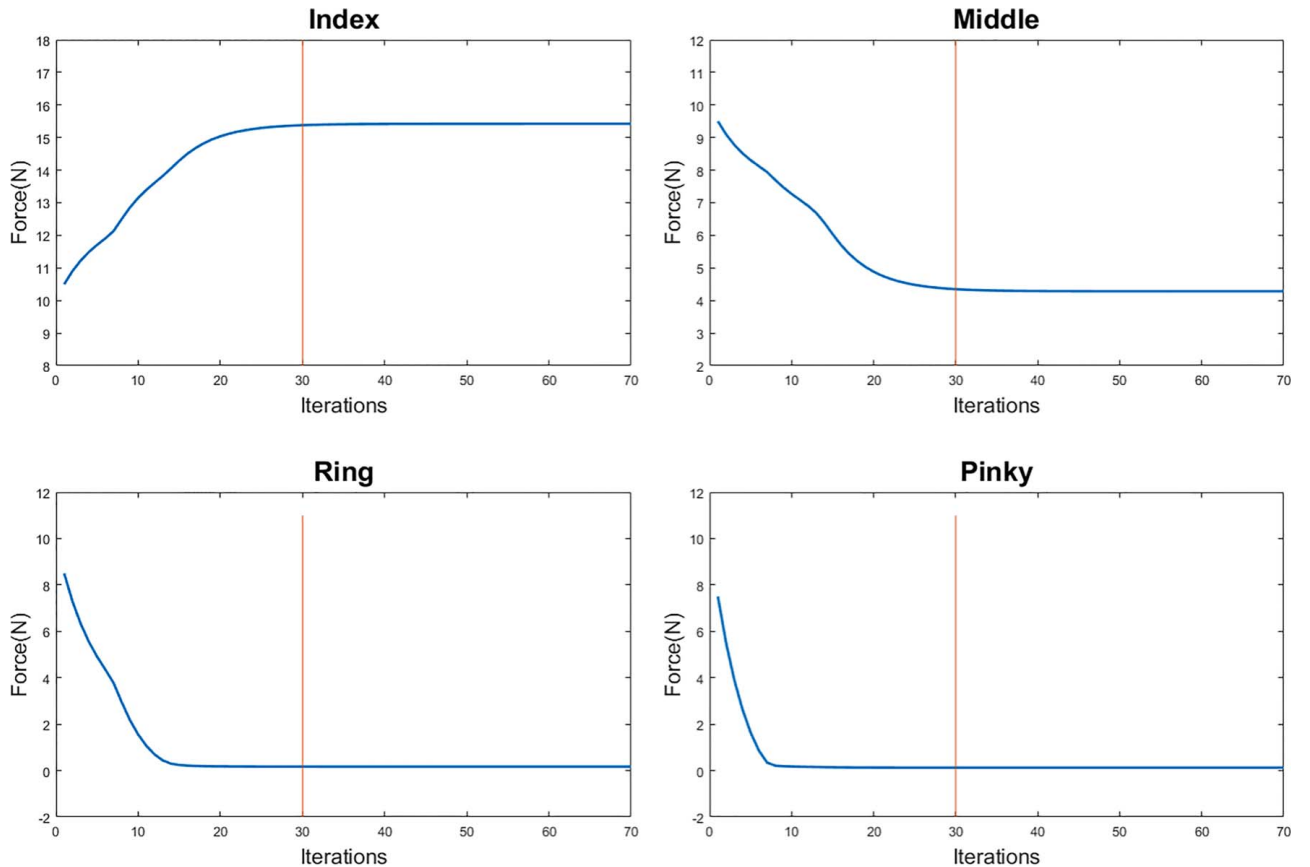
Fig. 6 Force convergence results of the optimization. Optimization used to generate the optimal set of forces for the four fingers is implemented initially on MATLAB and as can be observed the values converge to their optimal value in less than 30 iterations.
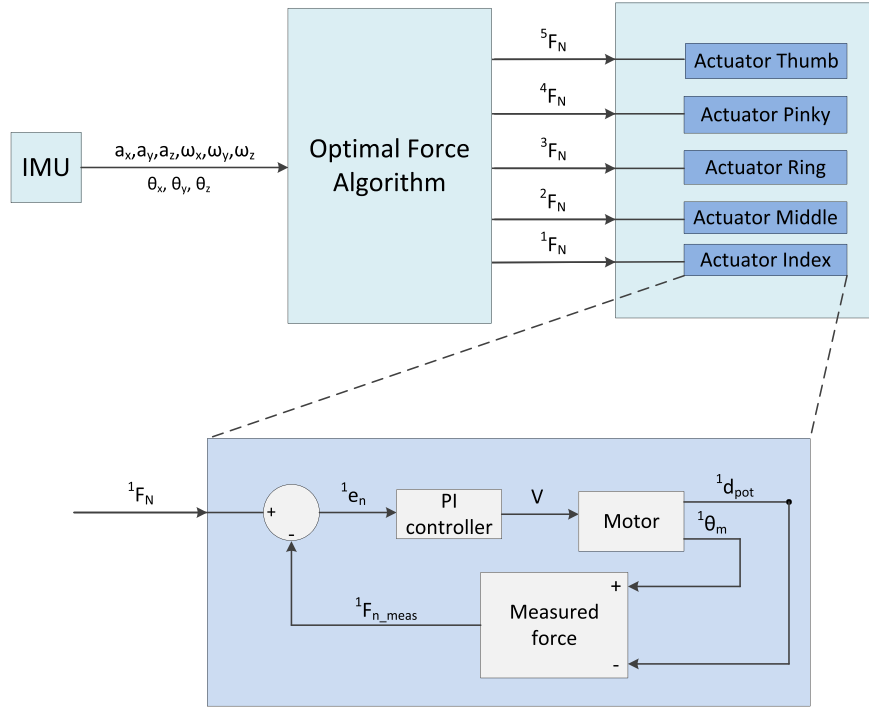
Fig. 7 Overall control architecture of the glove. This describes the data flow for this algorithm where data from the IMU are read by the algorithm and generates optimal set of forces. This optimal force values are sent to each actuator as a reference force which is tracked by the controller.

where P is the pitch of the leadscrew, N is the gear ratio of the gearhead of the motor, and k_s is the stiffness constant of the spring in the SEA.

The transfer function is used to build the feedback physical model in SIMULINK and is used to tune the PI gain parameters. The results of the tuned controller are briefly described in Table 2.

The force measured by the SEA is nonlinearly related to the force that is being applied at the tip of the finger where the object is being grasped. Therefore, a Jacobian transformation was applied to relate the force exerted by the SEA and the force applied at the fingertip. Equation (10) describes the relation between the input and output of the controller and the relation between the force measured by SEA and fingertip force

$$e_i = {}^iF_d - {}^iF_m \qquad i = 1, 2, 3, 4$$
$$ {}^iF_d = J_i{}^iF_N $$
$$ {}^iF_m = k_{spr}({}^id_{pot} - c^i\theta_m) \qquad (10)$$
$$ u_i = {}^ik_p e_i + {}^ik_{int} \int e_i dt $$

where ${}^iF_m$ is the measured force by the SEA, ${}^iF_d$ is the desired reference force by the SEA, k_{spr} is the SEA spring constant, ${}^id_{pot}$ is the linear potentiometer measurement, and ${}^i\theta_m$ is the motor position measured by the magnetic hall-effect encoder.

The Jacobian (J) for each finger is derived using the dynamics model developed in Ref. [2]. As can be seen, the dynamics model is highly nonlinear and its direct implementation on a microcontroller will pose computational issues. An approximate second-order polynomial model was fitted to the analytical dynamics model as shown in Fig. 9 and will be used in the Jacobian.

5 Prototype Integration

The RML glove was designed in SolidWorks and manufactured and integrated as shown in Fig. 10 to test both algorithms described

earlier. The glove base structure and most of the SEA parts including the screw-nut were manufactured using a 3D printer. The linkages were manufactured from a 0.8 mm thick aluminum sheet using a 2.5D milling machine so that it is sufficiently strong and lightweight. Direct current brushed motors were used with 250:1 gearbox that run on 12 V power supply with stall torque of 0.3 N m. For measuring the motor position, magnetic hall-effect encoders were used which provide 12 counts per revolution of motor shaft. The output of the SEA was measured using a linear potentiometer with 20 mm travel length. The actuators were controlled using teensy 3.6 microcontroller which also runs the deformation detection algorithm and optimal force algorithm. The microcontroller sends the motor pulse width modulation signals to the motor driver (by TI DRV8801), which can deliver a continuous current of 1 A and can operate between 8 V and 36 V.

MPU-9250 by InvenSense IMU was used for measuring the orientation and acceleration of the glove. It is a nine-axis motion tracking device that combines a three-axis magnetometer, three-axis accelerometer, and three-axis gyrometer. Magnetometer provides orientation of the device with respect to the magnetic north, the accelerometer provides the gravity and linear acceleration measurements along the three axes, and the gyrometer provides angular velocity about the three axes. Figure 11 describes the prototype along with all individual components used in building it.

Exponential smoothing method was used to remove noise from all the sensors including the IMU, linear potentiometer, and magnetic hall-effect encoders.

6 Experimental Setup and Results

6.1 Deformation Detection. In this test, a deformation detection algorithm was implemented and tested on the glove. Three different objects were selected with different stiffnesses for the test including a plastic water bottle, a polycoated paper cup, and a plastic cup.

Initial tests were carried out on these objects to quantitatively measure the stiffness of the objects. The test setup as shown in
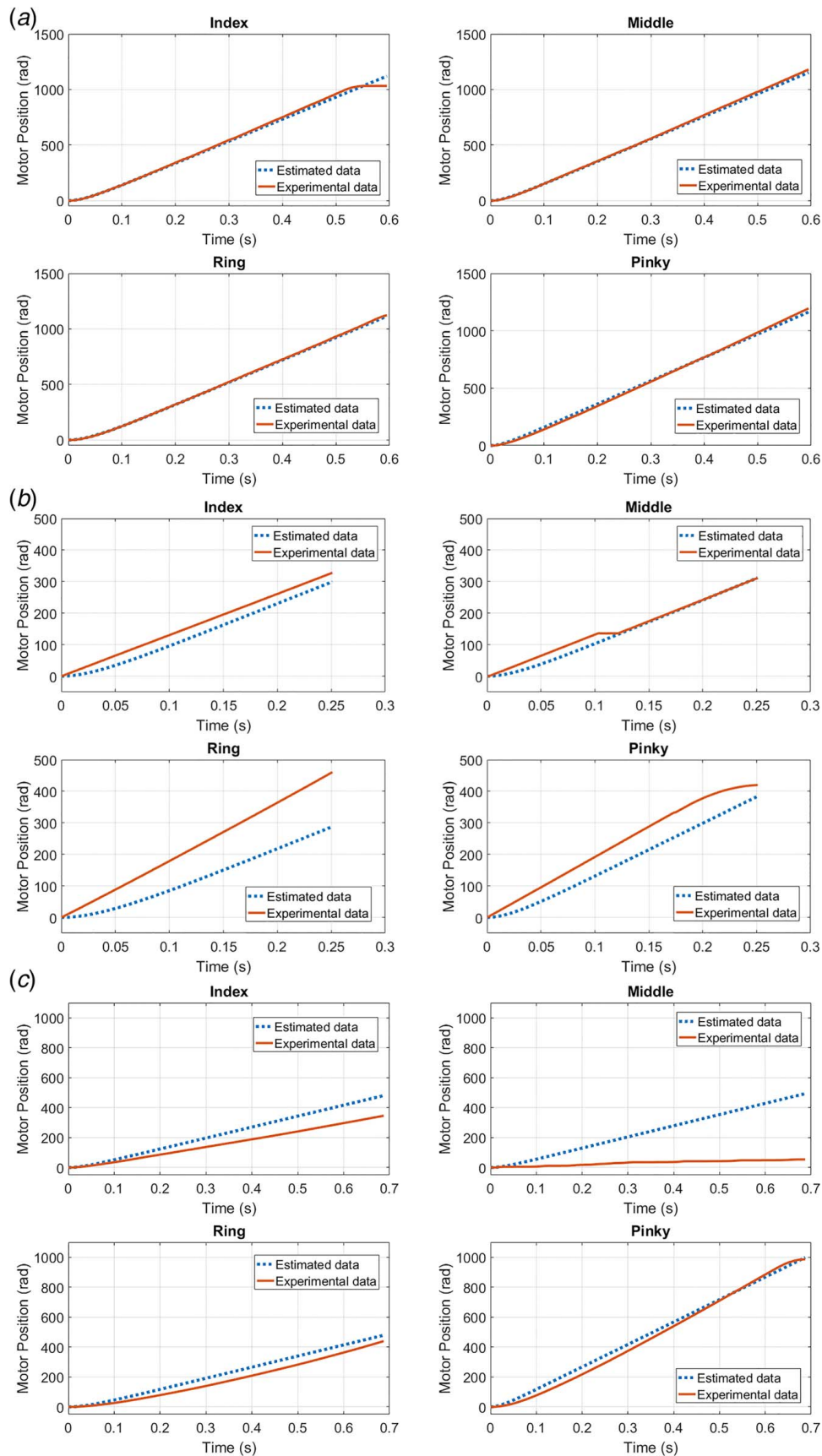
Fig. 8 Results of system identification of the four actuators. (*a*) Input voltage 8.2 V, (*b*) input voltage 5.6 V, and (*c*) input voltage 3 V. Second-order transfer function was estimated based upon the step response of the actuator. Estimation was performed in MATLAB. The inertia and viscous parameters are calculated by comparing the physical transfer function with the estimated transfer function.

Table 2   Tuned controller results

	Index	Middle	Ring	Pinky
Bandwidth (Hz)	1.42	1.52	1.47	1.22
Rise time (s)	0.17	0.16	0.15	0.2
Settling time (s)	0.27	0.27	0.23	0.37
Overshoot (%)	0.74	0.23	1.74	0.02

Fig. 10   RML glove prototype built to test the stable grasp algorithms including the deformation detection algorithm and optimal force algorithm

Fig. 12 includes a linear actuator with a force sensitive resistor (FSR) at its tip. The linear servo actuator was placed against the surface of the object such that it was slightly touching.

Then the linear actuator was commanded to move forward such that it pushes against the object while deforming it. The FSR was used to calculate the force applied by the linear actuator on the object and the potentiometer was used to calculate the distance traveled by the linear actuator which is also the deformation of the object. This test was carried out for all three objects and the results of the tests are depicted in Fig. 13. The measured data is fitted to a linear curve and is plotted along with it for comparison. By observation, it is clear that the plastic water bottle is stiffer than the poly coated paper cup which is also stiffer than the plastic cup. Since the stiffness properties of the objects were obtained, the subsequent tests with the glove were performed. The deformation detection algorithm was implemented and the deformation is measured. Initially the glove was positioned near the object to be grasped and all the linkages were fully extended so they are not touching the object. Then, constant velocity input was applied in a feedforward manner, such that the fingers start flexing and closing on the object. As soon as the finger makes contact with the object, the contact is detected based on the acceleration spike observed in the linear potentiometer measurements as shown in Fig. 14. The particular linkage upon making contact with the object halts the flexion and waits until all the fingers achieve contact. After all the fingers make contact, the deformation detection algorithm is engaged and the glove starts grasping the object with predefined forces. It is assumed that the user does not move the fingers until the deformation detection algorithm is engaged. But this requirement can be eliminated by using a reference force after the fingers make contact to readjust them in the event that the user may mistakenly move the fingers. While performing this grasp, the linear potentiometer and magnetic hall-effect encoder readings are measured and stored for analysis. This test was repeated for all three objects and all the measurements were stored. This test was repeated for all three objects with only the force
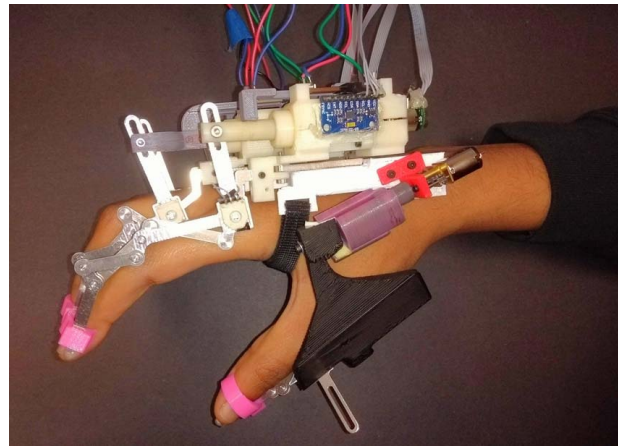
control implemented results that were used for comparison with the former test results.

As can be seen in Fig. 15, the plots are arranged in increasing stiffness of the object and the gap between the deformation for force control and deformation detection algorithm is decreasing with increasing stiffness as observed in the simulation results. This proves that the algorithm decreases the force applied proportional to the softness of the object.

6.2   Optimal Force Algorithm. Tests where the forces from the optimization are compared with forces produced by a human hand were performed. The test setup includes an object (water bottle) and four FSR sensors are attached on the bottle surface at known relative distances as shown in Fig. 16. An IMU is attached on the object at known distance from the region of grasp. Then the bottle is held by a healthy hand such that the four fingers are on top of the four FSR sensors. Three sets of experiments were performed: (1) hold the bottle in the air without any movement, (2) hold the bottle up and then translate in the direction of the force applied by the fingers back and forth three to four times, and (3) hold the bottle up and rotate the bottle in both clockwise and counter-clockwise direction.

While performing these tests, inertial data from the IMU and force data from the FSR are stored for post-processing. Hardware-in-loop
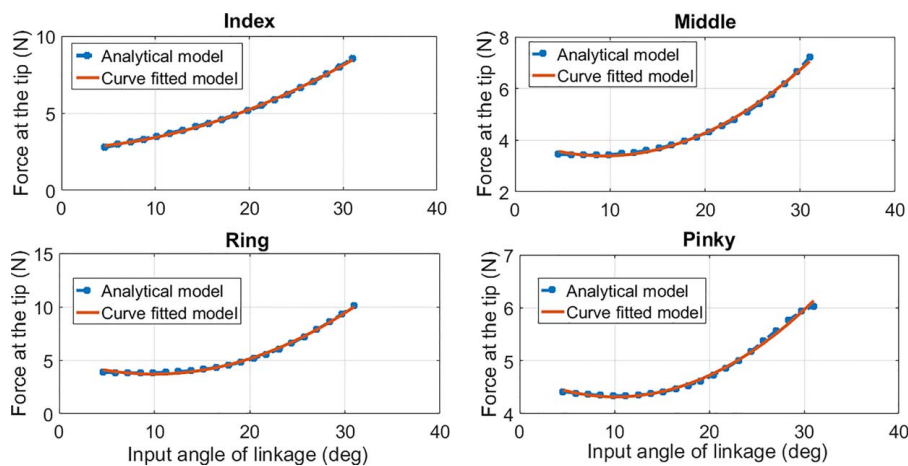
Fig. 9   Variation of tip force with joint angle. Here for a fixed input force of 15 N, the tip force is calculated analytically as the joint angle is increased. A second-order polynomial function is fitted to that analytic curve so that the polynomial function can be implemented in a microcontroller.
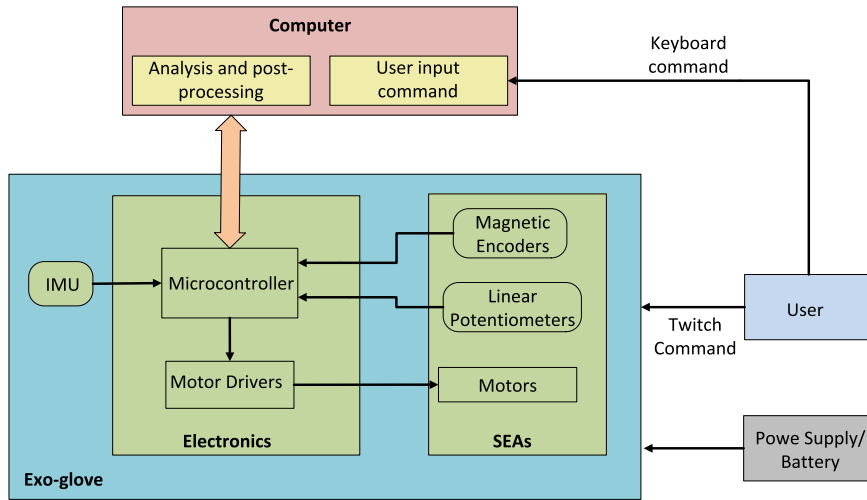
Fig. 11 Overall hardware architecture. The exoskeleton glove is communicating with a computer and the user for operation of the glove and analysis of data.

(HIL) simulation was performed where the data from the IMU was passed through the optimal force algorithm to generate the force distribution across the four fingers. Upon comparing the experimental data and the HIL simulation data as shown in Figs. 17–19; it can be observed that for all three cases the middle and ring finger forces match with greater accuracy. However, the pinky finger force had less matching pattern in terms of force magnitude. This test was done to check the ability of the algorithm in producing human like forces. It can be concluded that two out of four fingers exhibited acceptable matching in force magnitudes. The index finger matches partially with the experimental data and pinky finger demonstrates the lowest matching. This lower matching could be due to distribution of forces generated by the brain did not exactly follow the optimization method used, and even if it did, the objective function could be more complicated than the one used in the algorithm.

The algorithm was then implemented on the RML glove for testing. For the test, a water bottle was used as shown in Fig. 20 for grasping by the exoskeleton glove. Two tests were performed: (1) predefined grasp force was applied and the object was held stationary and (2) initially the object was lifted after applying a predefined grasp after which it was slowly rotated 90 deg clockwise and then back to the original position. The forces for each finger were determined by the optimization algorithm and the inertial data from the IMU.

From Fig. 21, it can be observed that all the fingers of the glove reach the desired force with a small steady-state error. The rise time is approximately 1.5 s which is due to motor and power limitations.

In the object rotation part of the test as shown in Fig. 22, the desired force is changing as it is rotated and the SEAs have
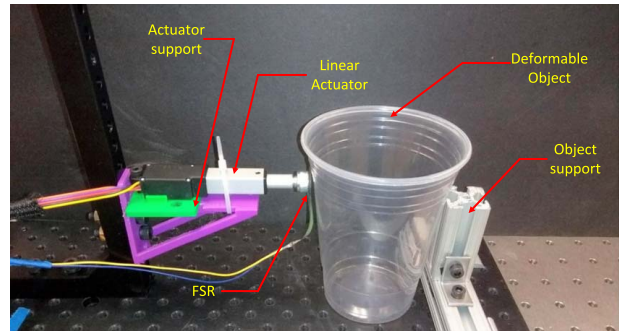

Fig. 12 Object material testing setup. This test setup was built to measure experimentally the stiffness of the three test objects using a linear actuator and FSR. These objects will be later used to perform the deformation detection test.
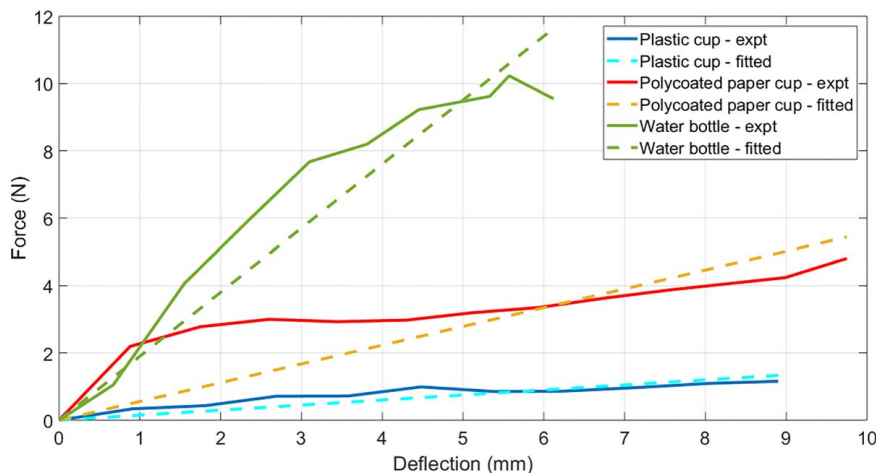

Fig. 13 Measured stiffness plot. Results of the material testing for the three objects are shown. A linear curve is fitted to the experimental plot and there is clear distinction between the stiffnesses of the three objects.
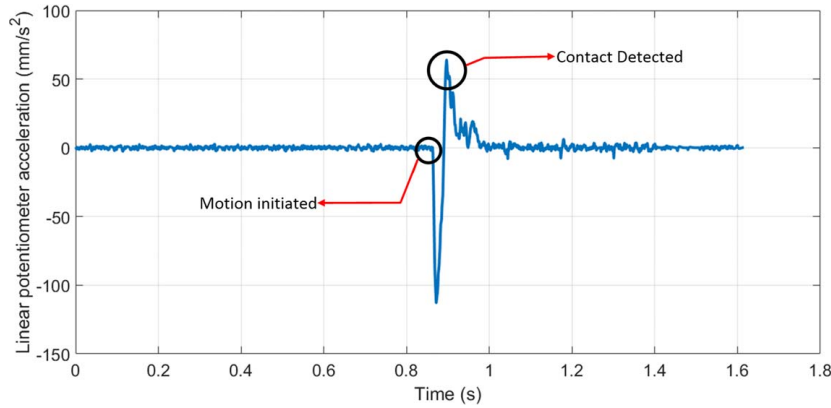
Fig. 14 Contact detection. The glove has initiated motion and upon contact with an object, there is a spike observed in the acceleration as measured by the linear potentiometer.
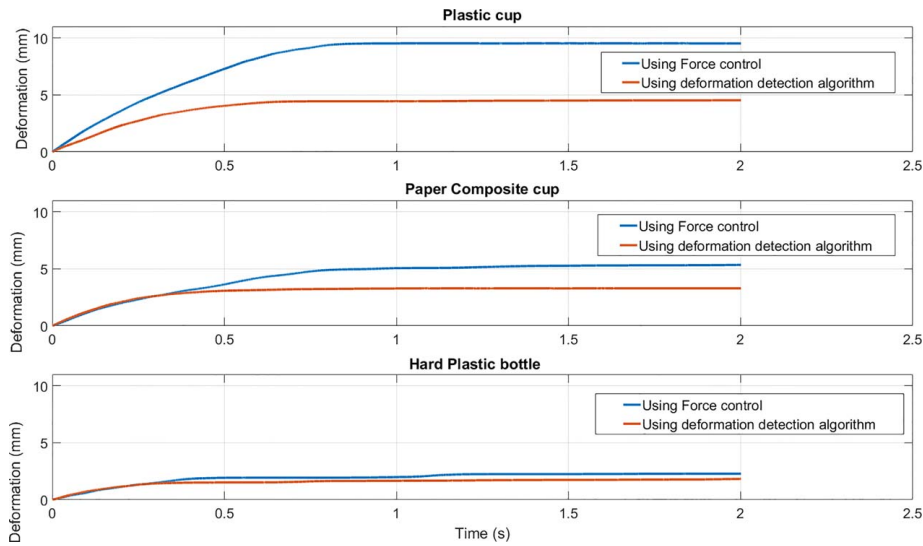
Fig. 15 Measured deformation algorithm response. The deformation detection algorithm is tested on the three objects and the linear potentiometer response is plotted against time. Response of the potentiometer when the algorithm is not implemented is also plotted for comparison.
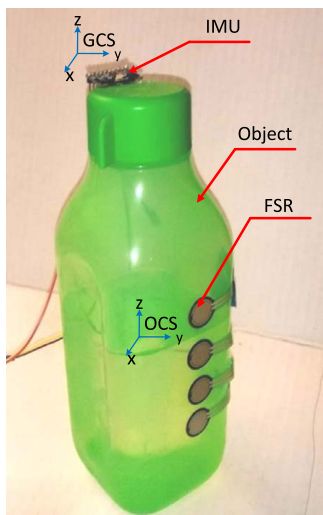

Fig. 16 Hand optimal test setup. This test setup was used to measure and compare the forces produced by human hand with forces generated by the optimization method.

approximately followed the profile. There was small delay between changes occurring in the desired force and the measured force which is due to motor velocity and power limitations as mentioned earlier.

7 Conclusion and Future Work

In this research, novel algorithms were developed which improve the grasp stability of an exoskeleton glove by using minimal number of sensors and low computational power. The algorithms helped improve the stability of grasp in two major ways: (1) detecting any deformation in the object while grasping and minimizing it, and (2) adjusting the force distribution among the fingers such that the force and moment equilibriums are maintained. Deformation is detected based upon tracking of the potentiometer and encoder readings and then decreasing the set point force value to prevent further deformation. The force optimal algorithm developed used information from the sensors and the IMU to calculate an optimal distribution of forces that satisfy the force and moment equilibriums. The Barrier method along with the infeasible start newton method was used for optimization and was implemented in a teensy microcontroller. It took 12 ms to run the optimization algorithm and was fast enough to have negligible errors. A full
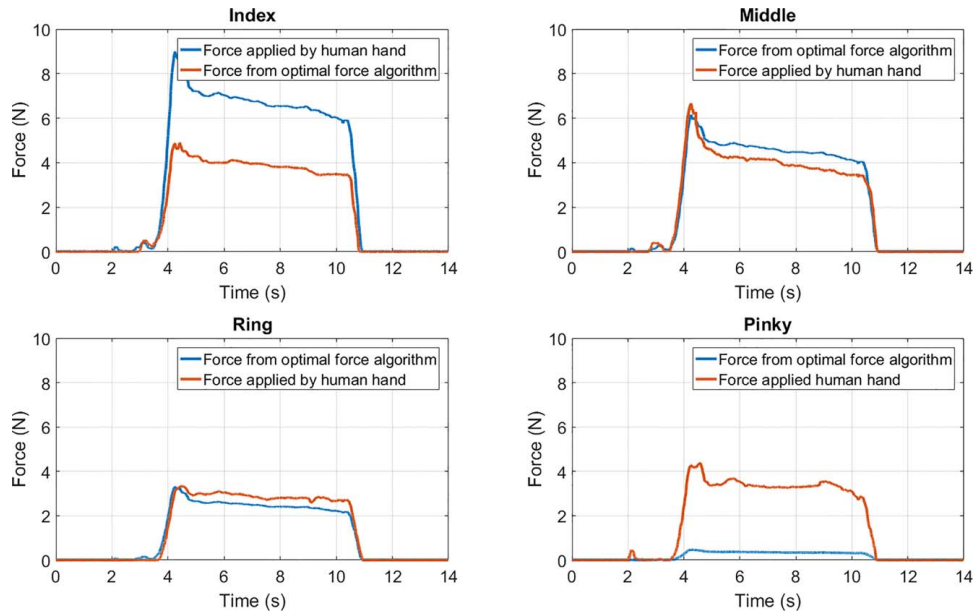
Fig. 17 Hand optimal test for holding. The forces generated by the human hand when grasping a bottle are compared with the forces as produced by the optimal force algorithm where the input is the total force produced by human hand. In this case the object is not being manipulated.

prototype was manufactured and integrated and was used to test and validate the proposed algorithms. The deformation detection algorithms implemented on the prototype produced similar results compared with the simulation. The glove was able to differentiate between objects with different stiffnesses and was able to reduce the deformation compared with when the algorithm was not implemented. The deformation reduction was higher for soft objects compared with rigid objects. Then the optimal grasp algorithm was implemented which, for known mass properties of the object, calculates the optimal forces for the four fingers. The thumb finger acted as a rigid support and provided a reaction force. Initial tests comparing the simulation results with a human hand showed a good match for two fingers and close similarity for the other two fingers. The glove performance was then tested for this algorithm.

Future research includes combining both algorithms so that they run simultaneously. Integration of rotary SEA or some other form of sensor for autonomous estimation of the mass of the object and other properties will be performed. Improvements in mechanical design of the glove will be performed such that it is lighter and more compact. Machine learning techniques can be applied to improve the performance of these algorithms. Further research can be performed by analyzing the computational cost, complexity, accuracy of the nonlinear constrained optimization method, results of which can be used to further improve the optimization method. In-depth study of friction characteristics needs to be performed to eliminate the delay issue and also experiment with different sliding materials in the linear actuator so as to have uniform friction characteristics that is not affected by the load, velocity, or position of the SEA. In addition, online stiffness measurement of the objects being grasped will be implemented using the sensor measurements after performing calibration tests so that the stiffness measured accurately represents the actual stiffness of the object.
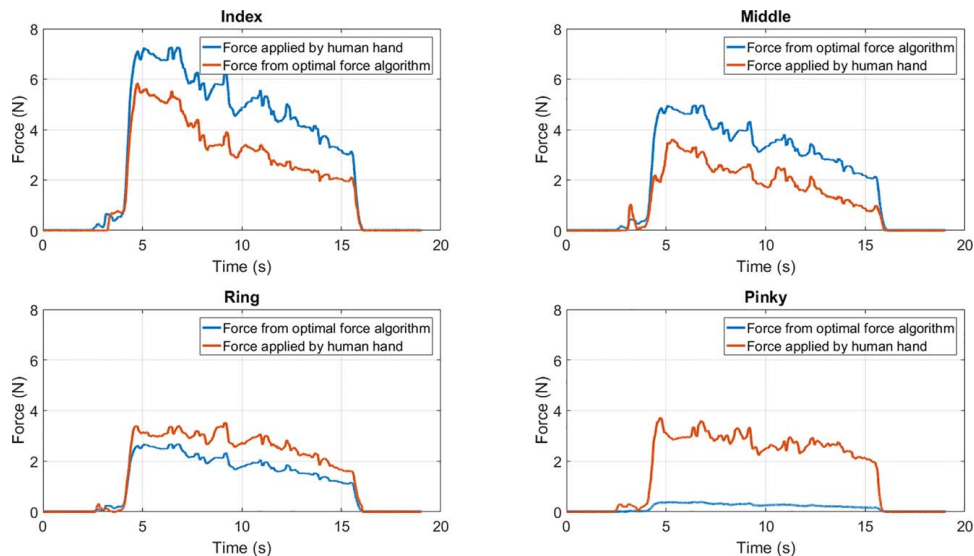

Fig. 18 Hand optimal test for translation. In this case the object was held and then translated in the horizontal direction in an oscillatory manner.
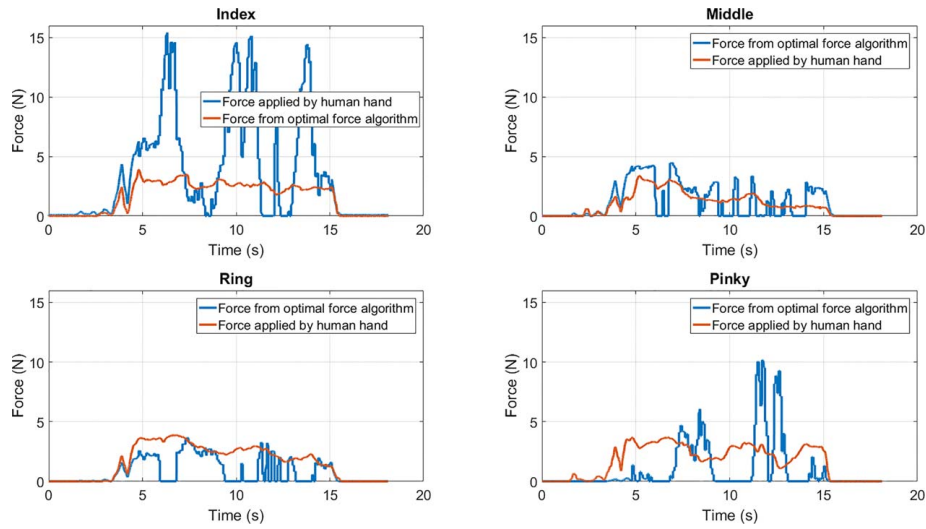
Fig. 19 Hand optimal test for rotation. In this case the object was held by hand then rotated in an oscillatory manner.

Fig. 20 Prototype glove shown here was used for testing the optimal force algorithm. The object in this case the water bottle is grasped and then the forces are applied as generated by the algorithm.
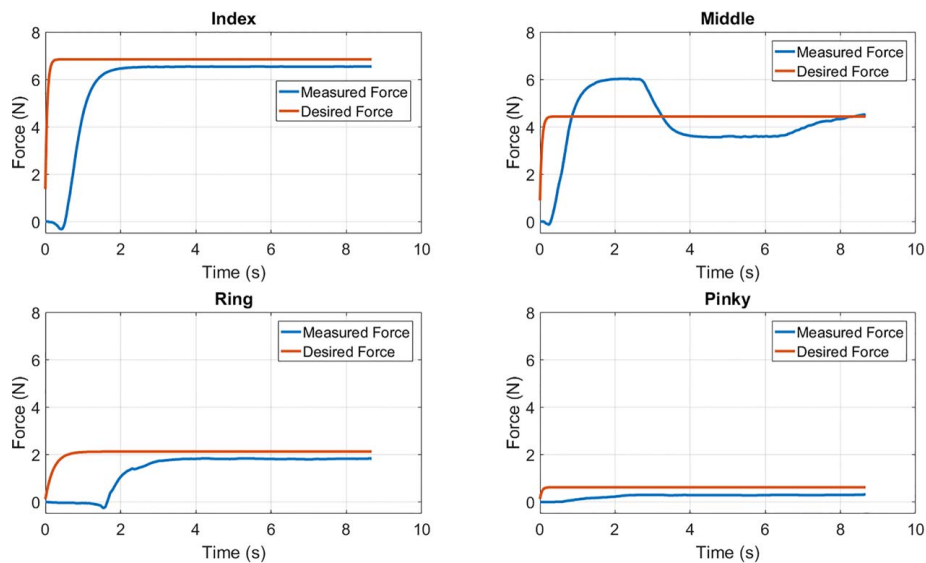
Fig. 21 Experimental results for holding are shown here where the object grasped is held stationary and no motion is imparted to the object. The desired force as generated by the optimization method is compared with actual force measured.
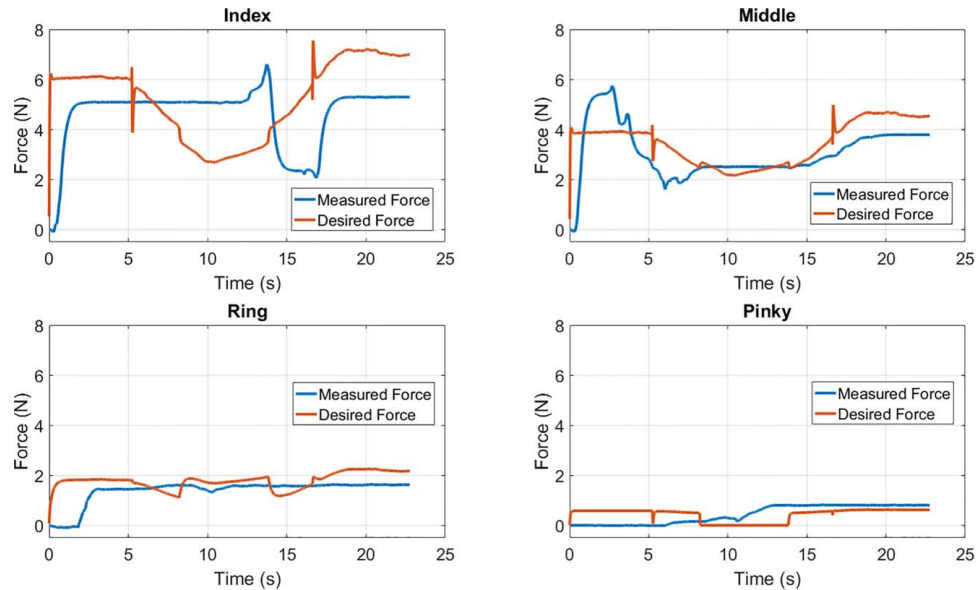
Fig. 22 Test results for rotation shown here for when the glove is grasping the object and then rotated about horizontal axis. The IMU measures the change in orientation and the optimization method generates the desired force profile as required.

Acknowledgment

Data Availability Statement

The authors attest that all data for this study are included in the paper. Data provided by a third party listed in Acknowledgment. No data, models, or code were generated or used for this paper.

References

[1] Refour, E., Sebastian, B., and Ben-Tzvi, P., 2018, "Two-Digit Robotic Exoskeleton Glove Mechanism: Design and Integration," ASME J. Mech. Rob., **10**(2), p. 025002.

[2] Vanteddu, T., Sebastian, B., and Ben-Tzvi, P., 2018, "Design Optimization of RML Glove for Improved Grasp Performance," Proceedings of the ASME 2018 Dynamic Systems and Control Conference (DSCC 2018), Atlanta, GA, Sept. 30–Oct. 3, pp. 1–8.

[3] Lee, S. W., Landers, K. A., and Park, H., 2014, "Development of a Biomimetic Hand Exotendon Device (BiomHED) for Restoration of Functional Hand Movement Post-Stroke," IEEE Trans. Neural Syst. Rehabil. Eng., **22**(4), pp. 886–898.

[4] In, H., Kang, B. B., Sin, M., and Cho, K., 2015, "Exo-Glove: A Wearable Robot for the Hand With a Soft Tendon Routing System," IEEE Rob. Autom. Mag., **22**(1), pp. 97–105.

[5] Nycz, C. J., Delph, M. A., and Fischer, G. S., 2015, "Modeling and Design of a Tendon Actuated Soft Robotic Exoskeleton for Hemiparetic Upper Limb Rehabilitation," 2015 37th Annual International Conference on IEEE Engineering in Medicine and Biology Society (EMBC), Milan, Aug. 25–29, pp. 3889–3892.

[6] Ben-Tzvi, P., Danoff, J., and Ma, Z., 2016, "The Design Evolution of a Sensing and Force-Feedback Exoskeleton Robotic Glove for Hand Rehabilitation Application," J. Mech. Rob., **8**(5), pp. 1–9.

[7] Iqbal, J., Khan, H., Tsagarakis, N. G., and Caldwell, D. G., 2014, "ScienceDirect A Novel Exoskeleton Robotic System for Hand Rehabilitation— Conceptualization to Prototyping," Integr. Med. Res., **34**(2), pp. 79–89.

[8] Agarwal, P., Fox, J., Yun, Y., O'Malley, M. K., and Deshpande, A. D., 2015, "An Index Finger Exoskeleton With Series Elastic Actuation for Rehabilitation: Design, Control and Performance Characterization," Int. J. Rob. Res., **34**(14), pp. 1747–1772.

[9] Howard, W. S., and Kumar, V., 1996, "On the Stability of Grasped Objects," IEEE Trans. Rob. Autom., **12**(6), pp. 904–917.

[10] Nakashima, A., Yoshimastsu, Y., and Hayakawa, Y., 2010, "Analysis and Synthesis of Stable Grasp by Multi-Fingered Robot Hand," IEEE International Conference on Control Application, Yokohama, Japan, Sept. 8–10, pp. 1582–1589.

[11] Lu, Y., Zhang, C., Cao, C., and Liu, Y., 2017, "Analysis of Coordinated Grasping Kinematics and Optimization of Grasping Force of a Parallel Hybrid Hand," Int. J. Adv. Rob. Syst., **14**(3), pp. 1–14.

[12] Bekiroglu, Y., Laaksonen, J., Jorgensen, J. A., Kyrki, V., and Kragic, D., 2011, "Assessing Grasp Stability Based on Learning and Haptic Data," IEEE Trans. Rob., **27**(3), pp. 616–629.

[13] Kinoshita, H., Murase, T., and Bandou, T., 1996, "Grip Posture and Forces During Holding Cylindrical Objects With Circular Grips," Ergonomics, **39**(9), pp. 1163–1176.

[14] Dang, H., and Allen, P. K., 2012, "Learning Grasp Stability," 2012 IEEE International Conference on Robotics and Automation, Saint Paul, MN, May 14–18, pp. 2392–2397.

[15] Kragten, G. A., Baril, M., Gosselin, C., and Herder, J. L., 2011, "Stable Precision Grasps by Underactuated Grippers," IEEE Trans. Rob., **27**(6), pp. 1056–1066.

[16] Suhaib, M., Khan, R. A., and Mukherjee, S., 2011, "Contact Force Optimization for Stable Grasp of Multifingered Robotic Grippers," World Congr. Eng., **III**, pp. 2194–2197.

[17] Haas-Heger, M., Iyengar, G., and Ciocarlie, M., 2018, "Passive Reaction Analysis for Grasp Stability," IEEE Trans. Autom. Sci. Eng., **15**(3), pp. 955–966.

[18] Lee, B. J. B., Williams, A., Ben-tzvi, P., and Member, S., 2018, "Intelligent Object Grasping With Sensor Fusion for Rehabilitation and Assistive Applications," IEEE Trans. Neural Syst. Rehabil. Eng., **26**(8), pp. 1556–1565.

[19] Chauhan, R. J., and Ben-Tzvi, P., 2018, "Latent Variable Grasp Prediction for Exoskeletal Glove Control," Proceedings of the ASME 2018 Dynamic Systems and Control Conference, Atlanta, GA, Sept. 30–Oct. 3, p. V001T07A002.

[20] Chauhan, R., Sebastian, B., and Ben-Tzvi, P., 2020, "Grasp Prediction Towards Naturalistic Exoskeleton Glove Control," IEEE Trans. Human-Mach. Sys., **50**(1), pp. 22–31.

[21] Howard, A. M., and Bekey, G. A., 2000, "Intelligent Learning for Deformable Object Manipulation," Auton. Rob., **9**(1), pp. 51–58.

[22] Cretu, A., Payeur, P., and Petriu, E. M., 2012, "Soft Object Deformation Monitoring and Learning for Model-Based Robotic Hand Manipulation," IEEE Trans. Syst. Man, Cybern. Part B, **42**(3), pp. 740–753.

[23] Drimus, A., Kootstra, G., Bilberg, A., and Kragic, D., 2011, "Classification of Rigid and Deformable Objects Using a Novel Tactile Sensor," 2011 15th International Conference on Advanced Robotics, Tallinn, June 20–23, pp. 427–434.

[24] Khalil, F. F., Payeur, P., and Cretu, A.-M., 2010, "Integrated Multisensory Robotic Hand System for Deformable Object Manipulation," IASTED Technology Conferences/705: ARP/706: RA/707: NANA/728: CompBIO, Cambridge, MA, Nov. 1–3, pp. 159–166.

[25] Delgado, A., Jara, C. A., Mira, D., and Torres, F., 2015, "A Tactile-Based Grasping Strategy for Deformable Objects Manipulation and Deformability Estimation," 2015 12th International Conference on Informatics in Control Automation and Robotics, Colmar, France, July 21–23, vol. 2, pp. 369–374.

[26] Huang, J., Todo, I., and Yabut, T., 2005, "Position/Force Hybrid Control of a Manipulator With a Flexible Tool Using Visual and Force Information," Cutting Edge Robotics, Pro Literatur Verlag, Germany.

[27] Boyd, S., and Vandenberghe, L., 2004, Convex Optimization, Cambridge University Press, Cambridge, UK.